ChemPubSoc Europe

DOI: 10.1002/celc.201300182

In Situ Electrochemical Generation of Mesostructured Cu_2S/C Composite for Enhanced Lithium Storage: Mechanism and Material Properties

Fei Han, Wen-Cui Li, Duo Li, and An-Hui Lu*[a]

An effective strategy is explored for the in situ generation of a Cu_2S/tubular mesoporous carbon composite by exploiting the charge–discharge processes of a S/C composite on a copper-foil current collector. By studying the reaction mechanism, we discover that the dissolved polysulfide ions (from the reaction of pristine sulfur) and inserted Li^+ are firmly anchored by the copper ions released from the copper foil, which forms insoluble Cu_xS intermediates in the mesopore channels of the carbon matrix. Moreover, the new electrochemically active Cu_xS intermediates are gradually converted to the final product, Cu_2S, during subsequent cycles. The as-prepared Cu_2S nanoparticles are highly dispersed throughout the tubular mesoporous carbon, and the Cu_2S/C composite exhibits a high reversible capacity of 270 mAh g^{-1} at 0.2 C over 300 cycles, with the negligible capacity loss, when used as a cathode material for a lithium-ion battery. Furthermore, the composite shows an outstanding rate capability with a reversible capacity of 225 mAh g^{-1} under a high rate of 10 C. This work provides a convenient platform for the controlled synthesis of metal sulfides for lithium-storage applications.

1. Introduction

Currently, lithium-ion batteries (LIBs) are the most utilized batteries in portable electronic devices because of their high energy density, light weight, and longer cycle life.[1–3] However, they are still unable to satisfy the fast-growing demand for high-capacity storage and fast charge–discharge processes, such as in electric vehicles and some high-power electric tools. The solution to meet the requirement is to develop new materials to overcome the limitation of conventional lithium-metal-oxide cathode materials based on intercalation reactions ($LiCoO_2$, $LiFePO_4$, and $LiMn_2O_4$, etc.).[4,5] Owing to the pioneering work towards various conversion-reaction compounds, high energy and power storage could be realized by utilizing all of the oxidation states of conversion-electrode cathode materials such as metal oxides,[6] sulfides,[7] fluorides,[8] and so forth.

Copper sulfides (Cu_xS), as a class of functional semiconductors with different phases, have numerous applications in the fields of optoelectronic device, sensors, solar cells and LIBs.[9–14] Among them, Cu_2S is considered to be a promising conversion-based cathode material for applications in low-voltage battery systems. Cu_2S has a high theoretical capacity (280 mAh g^{-1}), good electronic conductivity (ca. 10^4 S cm^{-1}), flat discharge curves, low fabrication costs, and can be produced from abundant resources in nature.[7,15,16] Moreover, owing to its high electronic and ion conductivity, Cu_2S cathodes can be fast-charged and discharged for high-power battery systems, rendering Cu_2S superior to other conversion-cathode materials such as FeF_3.[5,8,17] However, there have only been a limited number of studies using Cu_2S as a lithium-ion cathode material.[7,18] Therefore, the development of Cu_2S-based cathode materials to simultaneously improve the energy and power density of LIBs is of great importance, but remains very challenging. One of the major issues hindering the application of Cu_2S in LIBs is its poor cycle stability, mainly caused by reactive polysulfide intermediates, which can easily dissolve into organic electrolytes and migrate to the cathode, causing severe capacity decays.[18,19] Recently, studies in Li–S batteries have shown that porous carbon-decorated sulfur can effectively alleviate the escape of polysulfides from cathodes and improve the cycle stability.[20–23] Encouraged by this, fabrication of Cu_2S-encapsulated porous-carbon composites could be a promising solution for high-performance Cu_2S-based cathode materials. However, owing to the sophisticated preparation process of copper sulfide nanoparticles (< 10 nm), the preparation of highly dispersed copper sulfides encapsulated in a carbon matrix remains a challenge.

To date, in situ generation techniques have been employed to synthesize structure- and morphology-controlled nanomaterials. Previously, Lai et al.[7] developed a method for the direct growth of Cu_2S nanowire arrays on a Cu substrate by using a solution route; the electrode was found to deliver a specific capacity of 230 mAh g^{-1} and could maintain about 50% of the reversible capacity after 100 cycles. The cycle performance and rate capability of Cu_2S should be further improved to satisfy large-scale applications. Wang et al.[24] reported the in situ preparation of a nanoflake-like CuS cathode material on a Cu-foil substrate, which demonstrated a relatively stable cycle per-

[a] Prof. F. Han, Prof. W.-C. Li, D. Li, Prof. A.-H. Lu
State Key Laboratory of Fine Chemicals
School of Chemical Dalian University of Technology
Dalian, 116024 (PR China)
E-mail: anhuilu@dlut.edu.cn

Supporting Information for this article is available on the WWW under http://dx.doi.org/10.1002/celc.201300182.

 © 2014 Wiley-VCH Verlag GmbH & Co. KGaA, Weinheim

formance. However, the corresponding reaction mechanism, for the as-prepared CuS, during charge–discharge processes is not clear. Therefore, the in situ generation of high-performance Cu_2S cathode materials with excellent cycle stability and rate capability is essential, as well as an insight into the reaction mechanism.

Herein, we report the in situ generation of Cu_2S/tubular mesoporous carbon composite, which is produced through electrochemical charge–discharge-assisted processes. The tubular mesoporous carbon, with an open-pore structure, large pore volume, and thin walls, is regarded as an excellent carbon matrix for encapsulating various nanoparticles to improve lithium-storage performance, as indicated in our previous work.[25,26] The novelty of this work lies in the preparation method and the use of a different starting material and current collector. We use pristine sulfur as the starting material, which is encapsulated into the tubular mesoporous carbon, and a copper foil is employed as the cathode current collector instead of an aluminum foil (for loading the as-prepared S/C composite). During subsequent charge–discharge processes, we discover that the copper foil can be corroded (moderately) to release copper ions, which enable in situ anchoring of dissolved polysulfide ions through chemical interactions, thus, gradually generating new species, Cu_xS. As the charge–discharge cycles progress, the Cu_xS becomes an intermediate product and the final product of electrochemical oxidation–reduction is highly dispersed Cu_2S within the tubular mesoporous carbon. The Cu_2S/C composite displays good lithium-storage properties as a cathode material, with a stable cycle performance of 270 mAh g^{-1} after 300 cycles and a good rate capability of 225 mAh g^{-1} at 10 C.

2. Results and Discussion

2.1. Electrochemical Measurements

Galvanostatic charge–discharge cycling can provide straightforward evidence of the reactive electrochemical process in our system. The assembled S/C cell, with Cu foil as a current collector, was tested at a rate of 0.2 C between 1.0 and 3.0 V, and the representative charge–discharge voltage profiles are shown in Figure 1 a. During the first discharge process, two distinct voltage plateaus are clearly identified at 2.10 and 1.73 V. Two plateaus are also observed at approximately 1.85 and 2.25 V in the subsequent charge process. With increasing cycle numbers, the upper plateau (2.25 V) becomes shorter, and finally disappears after 20 cycles. In contrast, the lower plateau (1.85 V) becomes longer, and finally only one plateau at 1.85 V is observed in the charge curves. The discharge voltage profiles also show the same behavior, and the plateau develops to one (1.73 V). It is well known that the voltage profiles of elemental sulfur as cathode-active materials show typical two-plateau behavior, corresponding to the formation of long-chain polysulfides (Li_2S_x, $4 \leq x \leq 8$) at 2.3 V and short-chain Li_2S_2 and Li_2S at 2.1 V.[20,22,23] However, the voltage plateaus of active-sulfur cathodes remain almost unchanged during charge–discharge processes. Evidently, different voltage plateaus mean

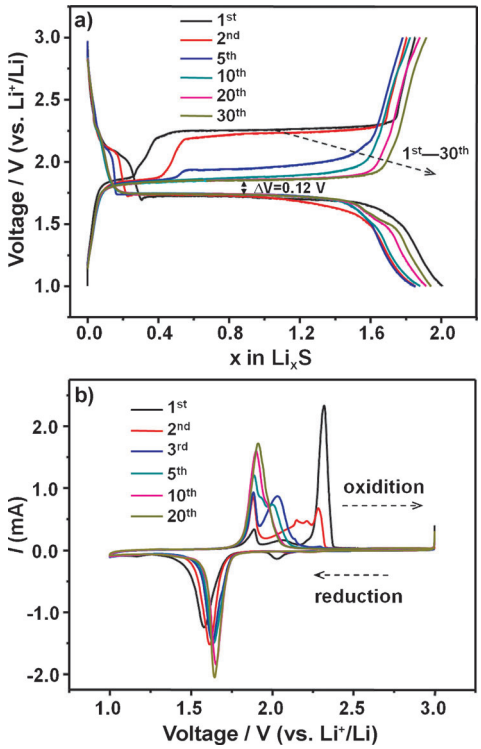

Figure 1. a) Representative charge–discharge voltage profiles and b) CVs of the electrode.

different electrochemical reactions. Hence, this is a strong indication that unusual reactions gradually occurred in the original S/C composite, with a Cu current collector, during the charge–discharge processes. Moreover, its final voltage plateaus are extremely flat and the voltage difference between the two plateaus is only 0.12 V, suggesting the existence of low kinetic barriers and superior reversibility of electrochemical reactions.[27,28]

Figure 1 b shows a typical cyclic voltammogram (CV) of one electrode at a scan rate of 0.2 mV s^{-1}. There are two obvious reduction peaks, occurring at approximately 1.60 and 2.05 V, which are attributed to the insertion of lithium, and two corresponding oxidation peaks at 1.88 and 2.32 V. The positions of the peaks correspond well to the typical plateaus in Figure 1 a. Similarly, the peaks at a higher voltage gradually disappear with increasing cycle number, and, finally, only a pair of peaks at lower voltage (1.60 and 1.88 V) can be observed. The results are consistent with the charge–discharge voltage profiles in Figure 1 a, but quite different from those reported for active-sulfur cathodes in the literature.[20–23,27,28] The possible mechanism was further investigated, as discussed below.

2.2. Structure and Properties of Electrode Materials after Cycling

To understand the reaction mechanism, we disassembled the spent cells in a glove box and washed the electrodes in dimethoxyethane (DME) to remove the residue of electrolyte. The electrodes were collected for further measurements. After dis-

© 2014 Wiley-VCH Verlag GmbH & Co. KGaA, Weinheim

assembly, it was observed that the color of the separator from the two cells with Cu- and Al-foil current collectors were white and dark yellow, respectively (see Figure S1 in the Supporting Information). The dark yellow residue on the separator originates from lithium polysulfides. This visually proves that almost no polysulfides escape from the composite when using a Cu foil as the current collector, indicating that the formed polysulfides are successfully anchored in the composite. Scanning electron microscopy (SEM) was employed to analyze the composition and morphology of the electrode after 30 cycles. As seen from the SEM image in Figure 2, the morphology of the tubular mesoporous carbon remains intact and no obvious agglomeration appears on the external of carbon matrix. Energy-dispersive X-ray (EDX) microanalysis confirms the existence of abundant Cu in the composite after cycling, and the Cu/S atomic ratio is 1.38. From the elemental mapping, it can be observed that the S and Cu elements are uniformly distributed throughout the carbon matrix.

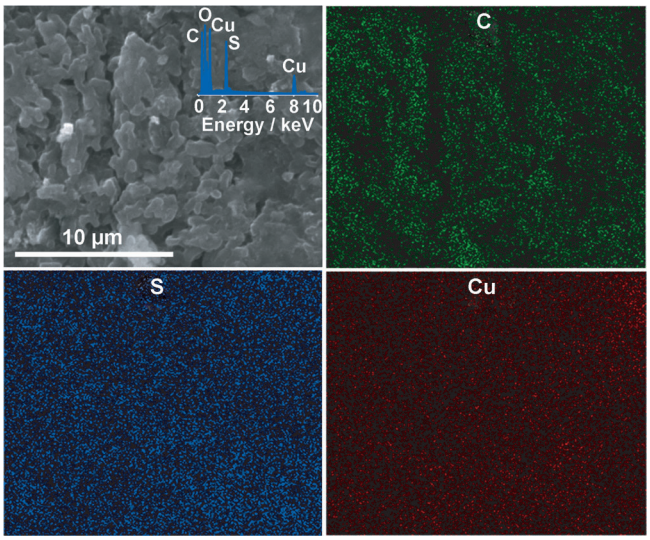

Figure 2. SEM image (inset: EDX spectrum) and the corresponding carbon, sulfur, and copper elemental mapping of the spent electrode material after 30 cycles.

To obtain more information, we carried out X-ray photoelectron spectroscopy (XPS) characterization on the electrode material after 30 cycles, as the XPS technique is a powerful tool for the detection of the element state. In Figure 3 a, the C 1s and O 1s peaks were examined in the wide-scan spectra of the pure carbon and S/C composite after 30 cycles. The spectrum of the latter shows obvious peaks of Cu 2p and relatively weak peaks for S 2p, according to the peak positions, which are in agreement with previous reports.[18,29] Figure 3 b reveals a stack-plot of XPS data for the Cu 2p core regions. Shake-up features at approximately 933 and 954 eV for the Cu $2p_{3/2}$ and $2p_{1/2}$ spin-orbit peaks are evident and diagnostic of the open $3d^9$ shell of Cu^+.[30,31] Besides these two main peaks, the weak shake-up satellite peaks at higher energy suggest the presence of Cu^{2+}.[30,31] Furthermore, the representative peak-fit of the Cu $2p_{3/2}$ peak reveals a main peak at 932.9 eV, which is accompanied by a series of satellites at 934.6, 940.7, and 942.9 eV (Figure 3 c).

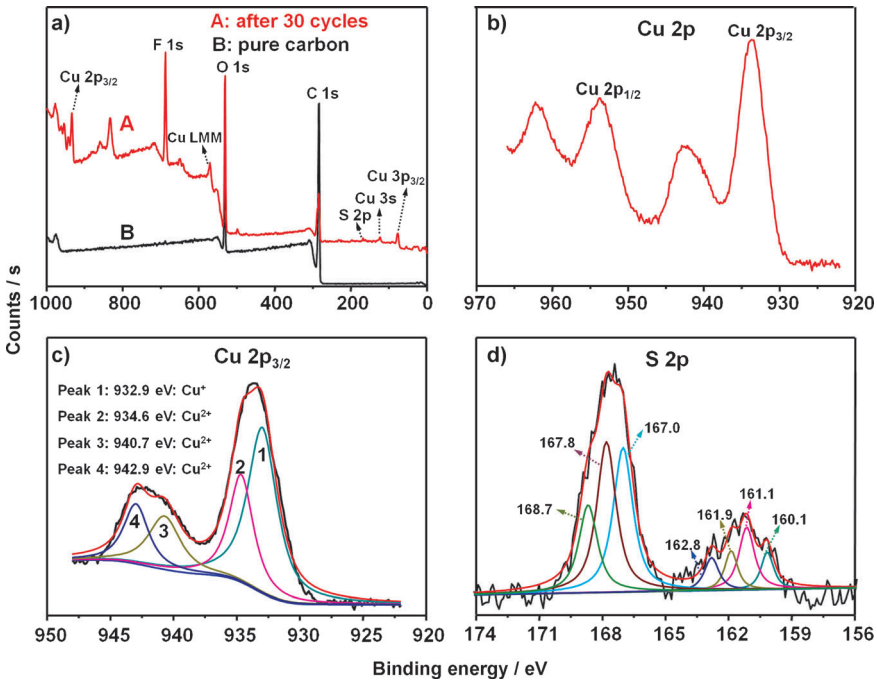

Figure 3. a) XPS survey of the pure carbon and the electrode material after 30 cycles. b) Cu 2p, c) Cu $2p_{3/2}$, and d) S 2p XPS analysis of the electrode material after 30 cycles. All XPS profiles were calibrated based on a C 1s binding energy of 284.6 eV.

The main peak is known as a characteristic of Cu^+ and peaks 2, 3, and 4 are assigned to the Cu^{2+} state.[30] The spectrum of the S 2p orbital (Figure 3 d) exhibits a higher complexity. Three main peaks positioned at 167.0, 167.8 and 168.7 eV indicate the existence of oxidized sulfur species, such as sulfonate, which could originate from the residual electrolyte salt (LiTFSI).[32] However, the two peaks at lower energy, 160.1 and 161.1 eV, are ascribed to unbound surface S_x^{2-} species.[29] Combining the results of the Cu 2p spectrum, the peaks at 161.9 and 162.8 eV correspond to S $2p_{1/2}$ for the Cu_2S (161.9 eV) and CuS (162.8 eV) phases.[18,33] Meanwhile, there are no distinct peaks in the range of 163.0–165.5 eV, implying the absence of elemental sulfur.[23,34] Overall, the XPS results indicate the presence of CuS and Cu_2S components and the absence of elemental sulfur in the electrode materials after 30 charge–discharge processes.

© 2014 Wiley-VCH Verlag GmbH & Co. KGaA, Weinheim

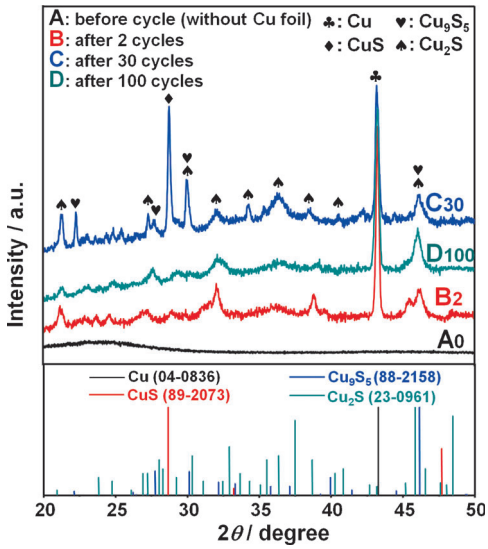

Figure 4. XRD patterns of the electrode before cycling (a), after two (b), after 30 (c), and after 100 (d) cycles in a charging state. The black, red, blue, and dark cyan vertical bars correspond to references of Cu (JCPDS No. 04-0836), CuS (JCPDS No. 89-2073), Cu_9S_5 (JCPDS No. 88-2158), and Cu_2S (JCPDS No. 23-0961) phases, respectively. The Cu peaks were attributed to the Cu-foil current collector.

Subsequently, the change of composition and structure of the active electrode materials before and after cycling is determined by using X-ray diffraction (XRD) measurements. As shown in Figure 4, the XRD pattern before cycling shows no obvious diffraction peaks, indicating a good dispersion of sulfur in the carbon matrix.[21] After two cycles, peaks corresponding to Cu_2S (JCPDS No. 23-0961) appear, accompanied by weak peaks reflecting the presence of Cu_9S_5 (JCPDS No. 88-2158) and CuS (JCPDS No. 89-2073). The XRD pattern of the sample after 30 cycles shows that the intensity of the CuS peaks become stronger and the peaks corresponding to Cu_9S_5 and Cu_2S are also observed. Combining these observations with the EDX results, the molar ratio of CuS/Cu_2S is 1.63, without considering the intermediate phase Cu_9S_5, which implies that CuS is the major component in the Cu_xS compounds after 30 cycles. Interestingly, after 100 cycles, the XRD pattern of the sample is similar to that after two cycles, suggesting that the major component, CuS, is converted into Cu_2S between 30 and 100 cycles. The results of the XRD measurements reveal that the final active electrode material is Cu_2S in the carbon matrix. However, the results also indicate that the atomic ratio of Cu/S in a fully delithiated state is first decreased and then increased within 100 cycles; this will be discussed in the following section.

Transmission electron microscopy (TEM) was further used to examine the morphology and properties of the formed Cu_xS/C composite. As shown in Figure 5, the mesostructures remain intact and stable after cycling. The edges of the composite are smooth and no bulky aggregates are visible. This strongly indicates that the newly formed Cu_xS particles are highly dispersed in the pore channels, rather than migrating to the external surface of the carbon matrix. Compared with the TEM images of original S/C composite (Figure S2 in the Supporting Information), it can be seen that the new Cu_xS products are formed in situ and replace the pristine sulfur particles in the mesopore channels of the carbon matrix.

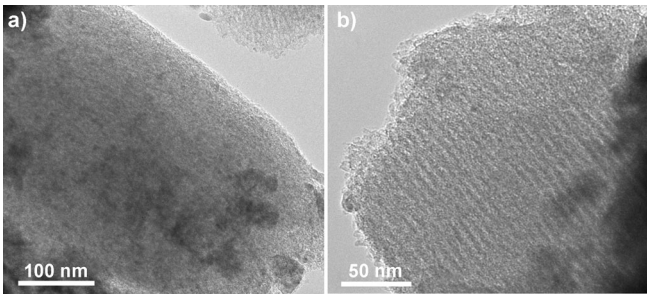

Figure 5. (a) TEM and (b) magnified TEM images of the electrode material after 30 cycles.

2.3. Mechanistic Insights

Considering the abovementioned results and previous studies, we attempted to deduce the electrochemical reaction mechanism of S/C to Cu_xS on the Cu foil in our system. The electrolyte salt (LiTFSI) is a Lewis acid that can corrode the Cu-foil current collector to release soluble Cu^+.[35,36] In our system, the formed Cu^+ is physically adsorbed by the residual pore channel of the S/C composite, owing to the large pore volume of the pristine carbon matrix.[37] During the first discharge process (voltage >2.10 V), the active external sulfur species (S_8) reacts with Li^+, leading to lithium polysulfide (Li_2S_n, $2<n\leq 8$).[20,22,23] Once the external S_n^{2-} dissolves into the ether-like solvent, Cu^+ rapidly and spontaneously reacts with S_n^{2-} to form insoluble Cu_2S_n compounds, owing to the extremely low solubility product constant [e.g. $K_{sp}(Cu_2S)=1.0\times10^{-48}$].[31,38] Consequently, the nanoparticles are encapsulated in the pores rather than distributed on the external surfaces of the carbon matrix, as evidenced from TEM observations. Fortunately, Cu_2S_n is a good electronic and ionic conductor (the electronic conductivity is ca. 10^4 S cm^{-1})[16,18] and can allow insertion of Li^+ to further react with active internal sulfur. Meanwhile, the restriction effect of external Cu_2S_n and the adsorption capacity of carbon also prevents the escape of S_n^{2-}. These reaction processes are rapid, so that no obvious voltage plateau can be seen over 2.10 V during the first discharge process:

$$Li_2S_n + (2n-2)\,Li^+ + (2n-2)\,e^- \rightarrow n\,Li_2S \quad (1)$$

$$Cu_2S + 2\,Li^+ + 2\,e^- \rightarrow 2\,Cu + Li_2S \quad (2)$$

$$Cu^+ + e^- \rightarrow Cu \quad (3)$$

$$Cu_2S + Li_2S - 2e^- \rightarrow 2\,CuS + 2\,Li^+ \quad (4)$$

When reaching the first plateau (2.10 V), internal Li_2S_n is further reduced to Li_2S following Equation (1), and external Cu_2S_n is reduced to the Cu_2S product. Subsequently, Li^+ reacts elec-

© 2014 Wiley-VCH Verlag GmbH & Co. KGaA, Weinheim

trochemically with Cu_2S to form Cu and Li_2S during the second plateau around 1.73 V [Eq. (2)], which is in accordance with previous findings.[7,12] The excess Cu^+ then transforms into metal Cu on the surface of the complex product [Eq. (3)]. During the first charge process, the lower plateau (1.85 V) represents the reverse process of Equation (2), and the quantity of Cu_2S is more than that formed during the first discharge process. This is attrbuted to the reaction of Cu formed following Equation (3) and Li_2S from Equation (1). Subsequently, some Cu_2S is converted to CuS following Equation (4), which has been reported with a similar voltage plateau.[39,40] Furthermore, with an increase in cycle number, more CuS is formed until Li_2S is exhausted. This is responsible for the phase change between two and 30 cycles, as disclosed by the XRD analysis. Then, the residual Li_2S is converted to Li_2S_n at the upper plateau of 2.25 V, and is further oxidized to S_8. During this process, the Cu-foil current collector is oxidized, leading to the release of Cu^+,[41] which can be observed in the CVs and SEM images of the bare Cu foil (Figure S3 and S4 in the Supporting Information). With the increase in Cu^+ content, the reaction shown in Equation (1) continuously fades, and the process described in Equation (2) flourishes during the coming cycles until the cease of the reaction shown in Equation (1). This accounts for the gradual change of the voltage plateau in Figure 1a. At this moment, the reaction presented in Equation (1) is also complete. Nevertheless, with the increase in Cu metal content, which originates from the reduction of Cu^+, CuS is gradually converted into Cu_2S during the charge–discharge processes. This is responsible for the increase in the atomic ratio of Cu/S, as seen in the XRD measurements. Together with the increasing amount of Cu_xS, which results in better electrochemical reactivity of the electrode, the specific capacity gradually increases with subsequent cycles, as shown in Figure 1a.

Finally, to further test the practicability of the proposed reaction mechanism, a transition-metal current collector, Ni foam, was also employed for loading the same S/C composite. The results demonstrate similar electrochemical behavior to that using a Cu-foil current collector (Figure S5 in the Supporting Information).

2.4. Electrochemical Characterization

It has been shown that the final electrochemically active component, Cu_2S, takes the place of pristine sulfur as the active cathode material. To prove the superiority of such an in situ-prepared Cu_2S/C composite cathode for rechargeable LIBs, we investigated the electrochemical properties of such electrode materials. Previously reported Cu_xS electrodes suffer from severe capacity fading during a long-term cycling, which is derived from the high solubility of higher order polysulfide anions, with S_n^{2-} ($2 < n \leq 8$) formed as reaction intermediates during a charge–discharge process.[7,12,19] Firstly, the cycle performance, together with the Coulombic efficiencies of such electrodes, are depicted in Figure 6a at a constant rate of 0.2 C

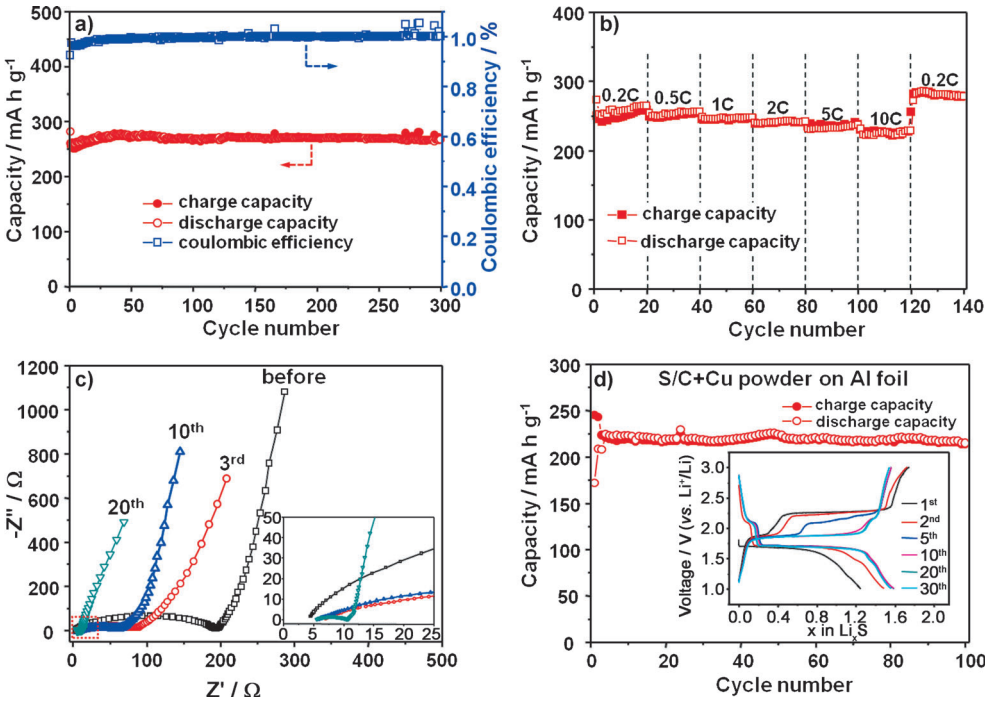

Figure 6. a) Long-term cycle performance and b) rate capability with increasing current density of the electrode. c) EIS Nyquist plots of the electrode before and after different cycle numbers (inset is the enlarged spectrum of dotted rectangle). d) Cycle performance of the mixture of S/C composite and Cu powder with an Al-foil current collector (inset is the representative charge–discharge voltage profiles).

(1 C = 337 mA g^{-1}) between 1.0 and 3.0 V. For comparison, the specific capacity was calculated on the basis of the total mass of Cu_2S and carbon in the final product. Interestingly, it is observed that, from the second to the fiftieth cycle, the capacities of the electrode increase continuously from 260 to 276 mA h g^{-1}, suggesting an increased utilization of active material, which has been explained above.

The high reversible capacity of 270 mA h g^{-1} can be maintained within 300 cycles without any apparent capacity loss, indicating the excellent cycle stability. To the best of our knowledge, the cycle stability is superior to those Cu_xS cathodes reported to date.[7,12,24] Moreover, the initial Coulombic efficiency is as high as 92%, which is higher than other nanoscale electrode materials. After the tenth cycle, the Coulombic efficien-

© 2014 Wiley-VCH Verlag GmbH & Co. KGaA, Weinheim

cies of the electrode materials are observed above 98%, indicating their good cycle reversibility. Such stable cycle performance and high Coulombic efficiencies indicate an excellent confinement effect of the carbon matrix for polysulfide ions, which is responsible for property deterioration.[12,19]

In addition, the high rate capability of such electrodes is shown in Figure 6b. With an increase in current rates, our cell only exhibits a slight decrease in capacity, but, eventually, a stable cycle capability is observed. For example, we notice a capacity drop of only 14% as the current rate increased from 0.2 to 10 C. The reversible capacity still remains at 225 mAh g^{-1} under a high rate of 10 C, suggesting rapid reaction kinetics, which is ascribed to the well-dispersed and highly conductive Cu_2S. The improved electrochemical properties are related to the internal resistance of the cathode, including bulk impedance and interfacial impedance, and are better understood by employing electrochemical impedance spectroscopy (EIS). The Nyquist plots, before and after cycling, were collected for comparison (Figure 6c). The depressed semicircle in the high/middle-frequency region represents charge-transfer resistance at the interface of the composite, and the oblique straight line in the low-frequency region corresponds to ion diffusion within the cathode.[26] Evidently, the interfacial charge-transfer resistance substantially decreases with increasing cycle numbers during 20 cycles. This indicates that the formed Cu_xS species has a higher electronic and ionic conductivity compared to pristine sulfur, and Cu_xS dramatically reduces the intrinsic resistance of the cathode. This observation agrees with the proposed reaction mechanism and may explain the enhancement in reversible capacity with subsequent cycles. Moreover, the resistance of the electrical contact, corresponding to the intercept at the real impedance axis in the high-frequency region, slightly increases from 4.5 (before) to 5.5 Ω after cycling (inset of Figure 6c). The negligible increase indicates that the electrical contact between the electrode material and the current collector is hardly affected by corrosion of the Cu foil. It should be pointed out that the low voltages of our cell partly overcompensate for the reasonable Coulombic storage densities.

Inspired by the reaction mechanism and excellent electrochemical performance, we physically mixed the S/C composite and Cu powder with an Al-foil current collector; the result is shown in Figure 6d. The cell shows almost the same cycle performance and charge–discharge voltage plateau change as that of the S/C composite pasted onto a Cu-foil current collector. This proves the rationality of the proposed reaction mechanism, and it also avoids the corrosion problems of current collector. More interestingly, such a reaction mechanism can be extended to guide the synthesis of other transition-metal sulfides, for example, NiS (see Figure S5 in the Supporting Information) and MoS_2, for superior electrochemical performance.

The flat voltage plateau, large reversible capacity, stable cycle performance, and excellent rate capability render the electrode a promising candidate as a cathode material for high-performance LIBs. The proposed electrochemical reactions occurring at the electrode during charge–discharge processes are suggested in Figure 7. Remarkably, our design allows soluble polysulfides to be anchored in situ by Cu^+ that is released through the corrosion of the Cu foil, which then forms insoluble Cu_xS intermediates [$K_{sp}(Cu_2S) = 1.0\times10^{-48}$, $K_{sp}(CuS) = 6.3\times10^{-36}$] on the surface of the sulfur. Importantly, the electrochemically active Cu_xS intermediates exhibit good electronic and ionic conductivity, and allow the insertion of Li^+ for further reaction with sulfur. With higher cycle numbers, the active sulfur is ultimately converted into Cu_xS compounds, which possess higher conductivity, better reversibility, and superior structure stability compared to pristine sulfur. Finally, with the increase in metal Cu content, the Cu_xS compounds completely transform to a single active material, Cu_2S. Furthermore, the unique structure of the electrode plays a key role in its long cycle stability. The in situ-formed Cu_xS particles are highly and homogeneously dispersed in the tubular mesopore channels of the carbon matrix. The advantages of such composite structure formed through in situ preparation have been reported in previous studies.[25,42] Moreover, the porous structure of the carbon matrix can effectively trap polysulfides and suppress their escape, thus improving the cycle stability of the electrode.

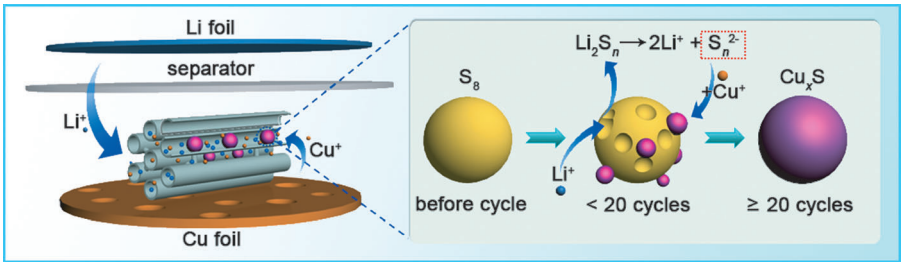

Figure 7. Electrode with firmly anchored polysulfide ions, which are held by the copper ions. Note: Cu_xS is an intermediate, not the final product.

3. Conclusions

We have demonstrated the in situ generation of a Cu_2S/tubular mesoporous carbon composite by using the charge–discharge processes of S/tubular mesoporous carbon on a Cu-foil current collector. The formed Cu_2S/C composite was employed as a cathode material, which exhibits long cycle stability and high rate capability. These properties can be attributed to the confinement effect of the carbon matrix and the high conductivity of the well-dispersed Cu_2S component. The proposed mechanism shows that the Cu foil, as the critical component, not only provides homogeneously distributed electron pathways,

© 2014 Wiley-VCH Verlag GmbH & Co. KGaA, Weinheim

but also releases copper ions to anchor the dissolved polysulfide ions. The entrapment ensures that elemental sulfur continuously converts to stable Cu_xS compounds. Moreover, the configuration is simple and feasible for large-scale applications, and opens up a new approach for the development of high-performance metal-sulfide cathode materials to be used in rechargeable LIBs. Further improvements in the action mechanism of this design, including the weight ratios of copper/sulfur, release rates of copper ions, effect of carbon hosts, as well as the cathode material design, are expected to extend the research field of rechargeable LIBs; work in this direction is underway in our laboratory.

4. Experimental Section

Synthesis of Cathode-Precursor Materials

Tubular mesoporous carbon was used as a matrix, which was synthesized as described in our previous reports.[43,44] The carbon matrix (0.1 g) was mixed with sublimed sulfur (0.166 g, Sinopharm Chemical Reagent Co.). The mixture was heated at 155 °C for 6 h in a sealed vessel under an argon atmosphere. Subsequently, the temperature was further increased to 300 °C for 1 h. After cooling to room temperature, the sulfur loading in the sulfur/carbon composite was approximately 50 wt%, which was calculated from the mass change between the pristine carbon and final composite.

Cell Fabrication and Electrochemical Measurements

Cu foil (35 μm in thickness), purchased from United Copper Foils (Huizhou) Ltd., was employed as the current collector. For comparison, Ni foam (1.59 mm in thickness) and carbon-coated Al foil (15 μm in thickness), obtained from Pylon Technologies, China, were also used. The current collectors were first pretreated. For example, the Cu foil was washed in acetone by ultra-sonication for 10 min, and the carbon-coated Al foil was rinsed with acetone. The electrode slurry was prepared by mixing 80 wt% of the composite material, 10 wt% of conductive carbon black, and 10 wt% of polyvinylidene difluoride (PVDF) binder in *N*-methyl-2-pyrrolidone (NMP) solvent. Subsequently, the electrode slurry was coated on top of the current collector and dried at 60 °C in vacuum for 15 h. The typical mass-loading of active sulfur was 0.7–1.0 mg cm^{-2}. CR2025-type coin cells were assembled with lithium foil as both the counter and reference electrodes in an argon-filled glove box. Celgard 2400 was used as a separator. The organic electrolyte solution was 1 M lithium bis(trifluoromethane sulfonamide) (LiTFSI) in 1,3-dioxolane (DOL) and dimethoxyethane (DME), with a volume ratio of 1:1. The galvanostatic charge–discharge measurements were conducted in a voltage window of 1.0–3.0 V by using a Land CT2001 A battery test system. The specific capacity was calculated based on the total mass of final Cu_2S and carbon, assuming the complete conversion of sulfur to Cu_2S. CV measurements and EIS were measured by using a CHI660D electrochemical workstation.

Physical Characterization

Morphological characterizations were carried out by using a FEI Nova NanoSEM 450 scanning electron microscope , and the EDX spectroscopy mapping was performed with an energy dispersive X-ray analyzer (Horiba EMAX). Surface analysis for the studied samples was performed on an X-ray photoelectron spectrometer (ESCALAB250) with a standard AlKα excitation source. The XPS spectra of all elements were referenced to the C 1s peak, arising from adventitious carbon (its binding energy was set at 284.6 eV). TEM investigations were carried out with a Hitachi HF2000 microscope equipped with a cold-field emission gun at a beam energy of 200 kV. XRD patterns were recorded between 20 and 50° at a scan rate of 0.5° min^{-1} on a Philips X-ray diffractometer, equipped with CuKα radiation to characterize the structures of the obtained composites.

Acknowledgements

The project was supported by the National Natural Science Foundation of China (No. 21225312 and 21376047), and the Ph.D. Programs Foundation (20100041110017) of the Ministry of Education of China.

Keywords: carbon · copper sulfide · lithium-ion batteries · mesoporous materials · reaction mechanisms

[1] N.-S. Choi, Z. Chen, S. A. Freunberger, X. Ji, Y.-K. Sun, K. Amine, G. Yushin, L. F. Nazar, J. Cho, P. G. Bruce, *Angew. Chem.* **2012**, *124*, 10134–10166; *Angew. Chem. Int. Ed.* **2012**, *51*, 9994–10024.
[2] S. Xin, Y.-G. Guo, L.-J. Wan, *Acc. Chem. Res.* **2012**, *45*, 1759–1769.
[3] M. V. Reddy, G. V. S. Rao, B. V. R. Chowdari, *Chem. Rev.* **2013**, *113*, 5364–5457.
[4] Y. Wang, G. Cao, *Adv. Mater.* **2008**, *20*, 2251–2269.
[5] D.-L. Ma, Z.-Y. Cao, H.-G. Wang, X.-L. Huang, L.-M. Wang, X.-B. Zhang, *Energy Environ. Sci.* **2012**, *5*, 8538–8542.
[6] S. Wang, S. Li, Y. Sun, X. Feng, C. Chen, *Energy Environ. Sci.* **2011**, *4*, 2854–2857.
[7] C.-H. Lai, K.-W. Huang, J.-H. Cheng, C.-Y. Lee, B.-J. Hwang, L.-J. Chen, *J. Mater. Chem.* **2010**, *20*, 6638–6645.
[8] S.-W. Kim, D.-H. Seo, H. Gwon, J. Kim, K. Kang, *Adv. Mater.* **2010**, *22*, 5260–5264.
[9] Y. Wu, C. Wadia, W. Ma, B. Sadtler, A. P. Alivisatos, *Nano Lett.* **2008**, *8*, 2551–2555.
[10] S.-C. Liufu, L.-D. Chen, Q. Yao, F.-Q. Huang, *J. Phys. Chem. C* **2008**, *112*, 12085–12088.
[11] Y. Du, Z. Yin, J. Zhu, X. Huang, X.-J. Wu, Z. Zeng, Q. Yan, H. Zhang, *Nat. Commun.* **2012**, *3*, 1177.
[12] Y. Chen, C. Davoisne, J.-M. Tarascon, C. Guéry, *J. Mater. Chem.* **2012**, *22*, 5295–5299.
[13] A. Hayashi, T. Ohtomo, F. Mizuno, K. Tadanaga, M. Tatsumisago, *Electrochem. Commun.* **2003**, *5*, 701–705.
[14] A. Hayashi, T. Ohtomo, F. Mizuno, K. Tadanaga, M. Tatsumisago, *Electrochim. Acta* **2004**, *50*, 893–897.
[15] K. D. Yuan, J. J. Wu, M. L. Liu, L. L. Zhang, F. F. Xu, L. D. Chen, F. Q. Huang, *Appl. Phys. Lett.* **2008**, *93*, 132106.
[16] P. Parreira, G. Lacareda, J. Valente, F. T. Nunes, A. Amaral, C. N. Carvalho, *Phys. Status Solidi A* **2010**, *207*, 1652–1654.
[17] T. Zhu, B. Xia, L. Zhou, X. W. Lou, *J. Mater. Chem.* **2012**, *22*, 7851–7855.
[18] R. Cai, J. Chen, J. Zhu, C. Xu, W. Zhang, C. Zhang, W. Shi, H. Tan, D. Yang, H. H. Hng, T. M. Lim, Q. Yan, *J. Phys. Chem. C* **2012**, *116*, 12468–12474.
[19] C. Xu, Y. Zeng, X. Rui, N. Xiao, J. Zhu, W. Zhang, J. Chen, W. Liu, H. Tan, H. H. Hng, Q. Yan, *ACS Nano* **2012**, *6*, 4713–4721.
[20] J. Schuster, G. He, B. Mandlmeier, T. Yim, K. T. Lee, T. Bein, L. F. Nazar, *Angew. Chem.* **2012**, *124*, 3651–3655; *Angew. Chem. Int. Ed.* **2012**, *51*, 3591–3595.
[21] C. Zhang, H. B. Wu, C. Yuan, Z. Guo, X. W. Lou, *Angew. Chem.* **2012**, *124*, 9730–9733; *Angew. Chem. Int. Ed.* **2012**, *51*, 9592–9595.
[22] X.-G. Sun, X. Wang, R. T. Mayes, S. Dai, *ChemSusChem* **2012**, *5*, 2079–2085.
[23] Y. Yang, G. Yu, J. J. Cha, H. Wu, M. Vosgueritchian, Y. Yao, Z. Bao, Y. Cui, *ACS Nano* **2011**, *5*, 9187–9193.

© 2014 Wiley-VCH Verlag GmbH & Co. KGaA, Weinheim

[24] Y. Wang, X. Zhang, P. Chen, H. Liao, S. Cheng, *Electrochim. Acta* **2012**, *80*, 264 – 268.
[25] F. Han, W.-C. Li, M.-R. Li, A.-H. Lu, *J. Mater. Chem.* **2012**, *22*, 9645 – 9651.
[26] F. Han, D. Li, W.-C. Li, C. Lei, Q. Sun, A.-H. Lu, *Adv. Funct. Mater.* **2013**, *23*, 1692 – 1700.
[27] G. Zheng, Y. Yang, J. J. Cha, S. S. Hong, Y. Cui, *Nano Lett.* **2011**, *11*, 4462 – 4467.
[28] Y.-X. Wang, L. Huang, L.-C. Sun, S.-Y. Xie, G.-L. Xu, S.-R. Chen, Y.-F. Xu, J.-T. Li, S.-L. Chou, S.-X. Dou, S.-G. Sun, *J. Mater. Chem.* **2012**, *22*, 4744 – 4750.
[29] M. Pang, H. C. Zeng, *Langmuir* **2010**, *26*, 5963 – 5970.
[30] M. Yin, C.-K. Wu, Y. Lou, C. Burda, J. T. Koberstein, Y. Zhu, S. O. Brien, *J. Am. Chem. Soc.* **2005**, *127*, 9506 – 9511.
[31] D.-F. Zhang, H. Zhang, Y. Shang, L. Guo, *Cryst. Growth Des.* **2011**, *11*, 3748 – 3753.
[32] J. P. Paraknowitsch, A. Thomas, J. Schmidt, *Chem. Commun.* **2011**, *47*, 8283 – 8285.
[33] S. Xiong, H. C. Zeng, *Angew. Chem.* **2012**, *124*, 973 – 976; *Angew. Chem. Int. Ed.* **2012**, *51*, 949 – 952.
[34] R. Demir-Cakan, M. Morcrette, F. Nouar, C. Davoisne, T. Devic, D. Gonbeau, R. Dominko, C. Serre, G. Férey, J.-M. Tarascon, *J. Am. Chem. Soc.* **2011**, *133*, 16154 – 16160.
[35] S.-T. Myung, Y. Hitoshi, Y.-K. Sun, *J. Mater. Chem.* **2011**, *21*, 9891 – 9911.
[36] L. Yang, M. Takahashi, B. Wang, *Electrochim. Acta* **2006**, *51*, 3228 – 3234.
[37] Z. Wu, W. Li, P. A. Webley, D. Zhao, *Adv. Mater.* **2012**, *24*, 485 – 491.
[38] S. J. Chadwell, D. Rickard, G. W. Luther, *Electroanalysis* **2001**, *13*, 21 – 29.
[39] A. Hayashi, T. Ohtomo, F. Mizuno, K. Tadanaga, M. Tatsumisago, *Electrochem. Commun.* **2003**, *5*, 701 – 705.
[40] A. Hayashi, T. Ohtomo, F. Mizuno, K. Tadanaga, M. Tatsumisago, *Electrochim. Acta* **2004**, *50*, 893 – 897.
[41] H. S. Choe, B. G. Carroll, D. M. Pasquariello, K. M. Abraham, *Chem. Mater.* **1997**, *9*, 369 – 379.
[42] F. Han, W.-C. Li, D. Li, A.-H. Lu, *J. Energy Chem.* **2013**, *22*, 329 – 335.
[43] A.-H. Lu, W. Schmidt, B. Spliethoff, F. Schüth, *Adv. Mater.* **2003**, *15*, 1602 – 1606.
[44] A.-H. Lu, W.-C. Li, W. Schmidt, W. Kiefer, F. Schüth, *Carbon* **2004**, *42*, 2939 – 2948.

Received: October 11, 2013
Published online on January 30, 2014

© 2014 Wiley-VCH Verlag GmbH & Co. KGaA, Weinheim